Energy Management System with Equalization Algorithm for Distributed Energy Storage Systems in PV-Active Generator Based Low Voltage DC Microgrids

Aldana, Nelson Leonardo Diaz; Hernández, Adriana Carolina Luna; Vasquez, Juan Carlos; Guerrero, Josep M.

Published in:
Proceedings of the 2015 IEEE First International Conference on DC Microgrids (ICDCM)

DOI (link to publication from Publisher):
10.1109/ICDCM.2015.7152057

Publication date:
2015

Document Version
Early version, also known as pre-print

Energy Management System with Equalization Algorithm for Distributed Energy Storage Systems in PV-Active Generator Based Low Voltage DC Microgrids

Nelson L. Díaz*†, Adriana C. Luna*, Juan C. Vásquez*, and Josep M. Guerrero*
*Department of Energy Technology, Aalborg University, Aalborg, Denmark
†Faculty of Engineering, Universidad Distrital F. J. C., Bogotá, Colombia
nda@et.aau.dk, acl@et.aau.dk, juq@et.aau.dk, joz@et.aau.dk
www.microgrids.et.aau.dk

***Abstract*—This paper presents a centralized strategy for equalizing the state of charge of distributed energy storage systems in an islanded DC microgrid. The proposed strategy is based on a simple algorithm called equalization algorithm, which modifies the charge or discharge rate by weighting the virtual resistor of local droop control loops at each distributed energy storage system. The proposed strategy, can be used as an additional function of the microgrid energy management system where the state of charge of distributed ESS is equalized within a determined window of time. Finally, real-time simulation results of a low voltage DC microgrid are presented in order to verify the performance of the proposed approach.**

***Keywords*—Distributed energy storage systems, Droop control, Equalization algorithm, State of Charge.**

I. Introduction

Low voltage DC power distribution systems have been widely used for supplying critical loads, such as data centers, remote communication stations or residential applications [1], [2]. In particular, DC power distribution systems offer more reliability, and efficiency than conventional AC power distribution systems [3]. In addition, aspects associated with synchronization, reactive power flow, and harmonic currents are not a concern in DC power systems [4].

With the fast development of Renewable energy sources (RES), a microgrid appear as a feasible solution for a coordinated integration of RES into a low voltage DC power system [5]. However, the stochastic behavior of the RES, such as photovoltaic (PV) generators, requires the integration of more energy storage systems (ESS) in order to smooth the variations at the RES [6]. As a matter of fact, when economic and environmental issues do not allow interconnection with the main power grid, the capacity of the ESS needs to be increased in order to ensure several to many hours of energy reserve [7]. For that reason, the current trend is oriented to the integration of distributed RES and its corresponding ESS as a unit denoted as active generator (PV+ESS) [6], [8]. Fig. 1 shows the basic scheme of an islanded DC microgrid composed by two (PV+ESS) active generators and a critical load. Commonly, valve regulated lead-acid (VRLA) batteries are the most used in islanded microgrids, since they offer

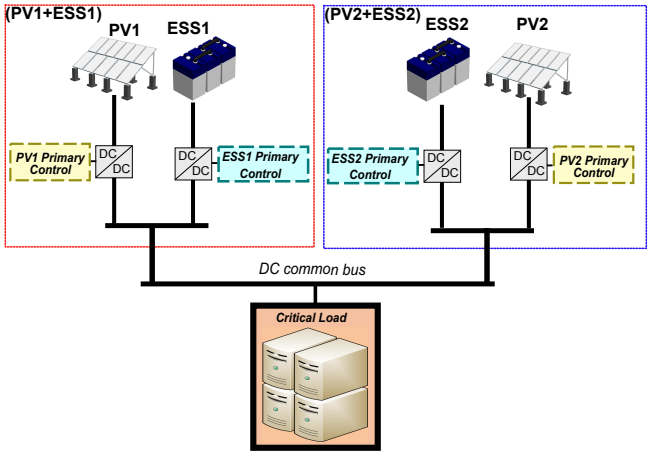

Fig. 1: Islanded DC microgrid configuration based on (PV+ESS) active generators.

a good commitment between energy density, deep-cycle life, transportability, availability, and cost [7], [9].

When distributed ESS are used, it is recommended a coordinated operation between them in order to avoid deep-discharge in one of the energy storage unit and over-charge in the others. Differences at the SoC could limit the life-time of the ESS with the smallest SoC, since this ESS will be exposed to bigger deep of discharge [10]. Therefore, when the ESS are being charged, it is desirable to prioritize the charge of the ESS with the smallest state of charge (SoC), and on the contrary, when the ESS are being discharged, the unit with the highest SoC should provide more power to the microgrid than the others in order to ensure stored energy balance [11], [12].

Commonly, droop control strategies are used in order to achieve good power sharing between units [5]. Indeed, conventional control loops for distributed ESS are complemented with control actions which adjust the droop coefficients in accordance to the SoC. In this way, it is possible to achieve equalization at the stored energy. It this sense, several different approaches have been proposed for equalizing the SoC at distributed ESS such as in [13]–[20]. However all of them assume equal capacity for all the distributed ESS. In [4], the authors consider some differences between energy storage

units. Despite this, the equalization strategy is applied to ESS based on electric-double-layer capacitors rather than on batteries. Although, the stored energy is balanced, long time and additional control loops are required.

This paper proposes a simple function for the energy management system (EMS) of an islanded DC microgrid, based on a centralized strategy denoted as equalization algorithm, which achieves asymptotic approach of the SoC within an established window of time for distributed ESS based on batteries. The proposed equalization algorithm weights the droop coefficients of the droop control loops, within a defined window of time, in order to equalize the SoC for distributed ESS. Real-time simulation results under charge and discharge conditions and considering differences at the batteries capacity are presented in order to validate the proposed strategy.

The paper is organized as follows. Section II explains the operation of the microgrid and how the droop control loops should be adjusted in order to achieve equalization. Section III explains the proposed equalization algorithm, and finally Sections IV and V present real-time simulation results and conclusions respectively.

II. Configuration and Operation of the DC Microgrid

The low voltage DC microgrid consider for this study-case is composed by two PV-based active generators (PV+ESS) and a critical load (see Fig. 1). The microgrid is formed around a standard $48V_{dc}$ common bus, which is a kind of low voltage DC power distribution system that is widely used, since it allows working on a live conductor with minimum risk for personal injury and without special safety requirements [21]. Moreover, non-isolated buck DC/DC converters operating in continuous mode are used for the conversion stage of each RES and ESS as proposed in [15].

In isladed operation, it is expected that the RES' operate by using a maximum power point tracking (MPPT) algorithm, in order to obtain from the RES the maximum amount of available energy. Fort that reason, RES' operate as constant power sources following the current reference given by the MPPT algorithms. This current reference can be obtained from MPPT methods as the one proposed in [22]. However MPPT strategies are out of the scope of this paper, interested readers may also refer to [23]. To get back to the point, the inductor current of the converter is controlled by typical inner current loops. Fig. 2 shows the scheme of the inner current control for each RES.

Meanwhile, the ESS operate in voltage control mode (VCM) being responsible of regulating the bus voltage. At this mode, the batteries will be charged or discharged in order to compensate the unbalance between the energy generated by RES and load consumption [20], [24]. Commonly, The power unbalance is equally shared between ESS by means of conventional droop control loop [5]. Therefore, the voltage at the common bus (V_{DC}) is established by the following equation:

$$V_{DC} = V_{DC}^{*} - Rd \cdot I_{ESSi} \tag{1}$$

where Rd is the virtual resistance of the droop control loop, V_{DC}^{*} is the voltage reference of the common DC bus, and

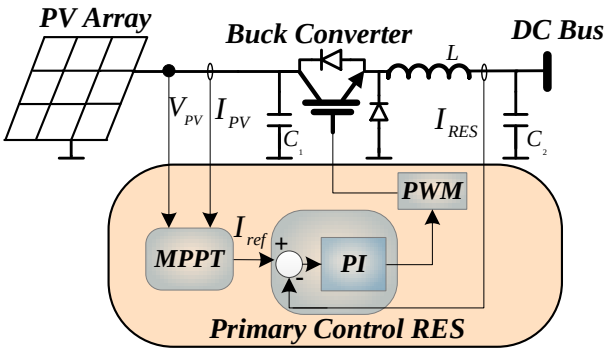

Fig. 2: Control diagram for RES.

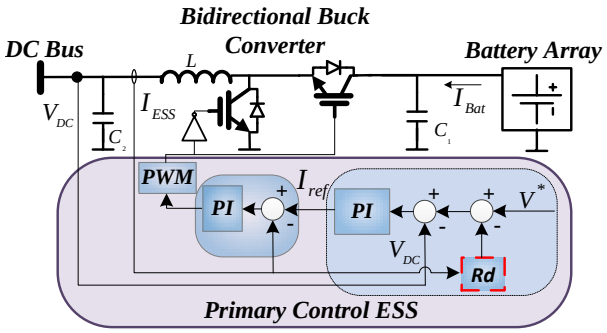

Fig. 3: Control diagram for ESS.

I_{ESSi} is the output current of each ESS. In this case, a typical double-loop VCM controller is implemented for a bidirectional non-isolated buck converter, as can be seen in Fig.3. When the same virtual resistance (Rd) is applied to each ESS control loop, the current is equally shared between ESS (see Fig. 4(a)).

Under the discharge of the battery, for balancing the SoC between ESS, the ESS with the highest SoC should supply more power to the microgrid than the other. On the contrary, when the batteries are being charged the ESS with the smallest SoC should get more energy from the microgrid than the other. This behavior can be achieved by weighting the virtual resistance (Rd) by a factor α_i as is shown in Fig. 4(b), where the largest SoC have been assumed for ESS2. Therefore, (1) can now be rewritten as follows:

$$V_{DC} = V_{DC}^{*} - Rd \cdot \alpha_i \cdot I_{ESSi} \tag{2}$$

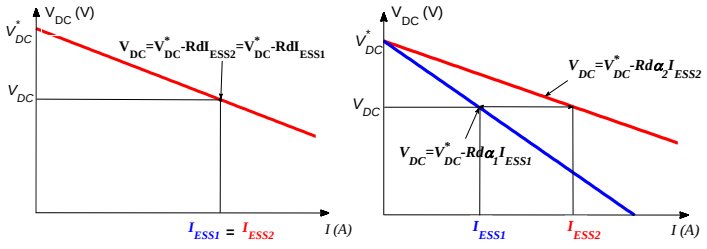

Fig. 4: Droop characteristics: (a) Equal virtual resistance Rd (b) Weighted virtual resistance αRd.

Finally, the microgrid system is complemented with an energy management system (EMS) that execute the equalization algorithm in order to obtain the values for α_1 and α_2 as can be seen in Fig. 5.

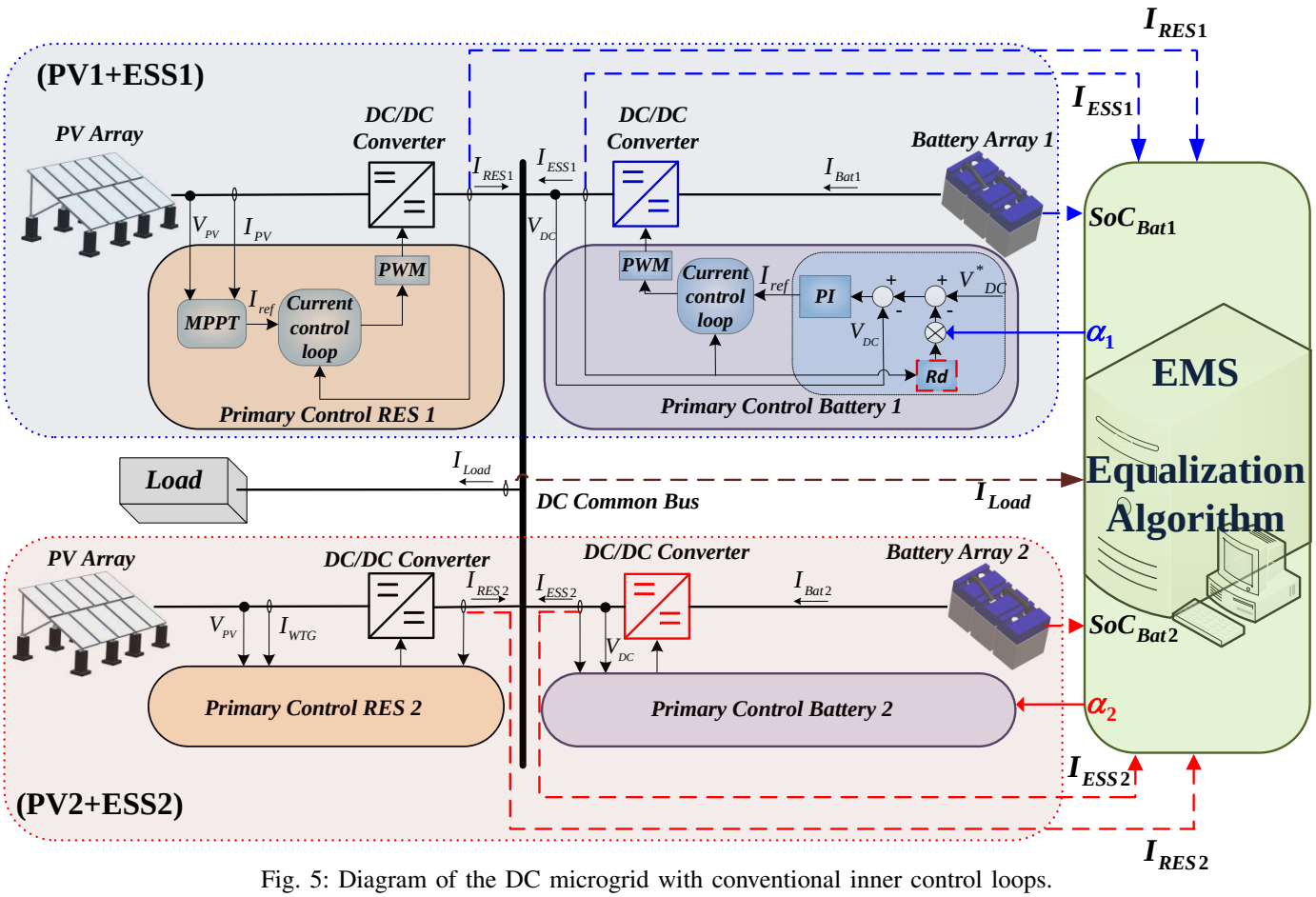

Fig. 5: Diagram of the DC microgrid with conventional inner control loops.

It is important to say that this paper will only consider the operation of the microgrid when the ESS are being charged or discharged. Anyhow, the operation of the microgrid should be complemented by appropriate charge strategies that avoid excessive overcharge in the batteries, such as in [20], and [15], as well as load-shedding, or actions for limiting the deep of discharge of the batteries as proposed in [25]. Next Section will explain the proposed equalization algorithm in detail.

III. Proposed Equalization Algorithm for SoC

The algorithm is based on the fact that the rate of change of the SoC is directly proportional to the battery current ($I_{bati} \propto m_{SoCi}$), where m_{SoCi} is the rate of change for the SoC at each ESS. For that reason, by adjusting m_{SoCi} it is possible to achieve an equalization of the SoC at distributed ESS, as is shown in Fig. 6, where the dashed lines represent the behavior of the SoC without compensation, and the continuous lines represent the expected behavior of the equalization algorithm.

In order to derive the proportional relationship between the battery current and the ration of the SoC, we consider the ampere-hour (Ah) counting method equation [15],

$$SoC(\Delta t)_{Bati} = SoC(0)_{Bati} - \int_0^{\Delta t} \eta_{Bati} \frac{I_{Bati}(\tau)}{C_{Bati}} d\tau \quad (3)$$

where $SoC(\Delta t)_{Bati}$ is the final SoC after a period Δt, $SoC(0)_{Bati}$ is the initial SoC, C_{Bati} is the capacity of the

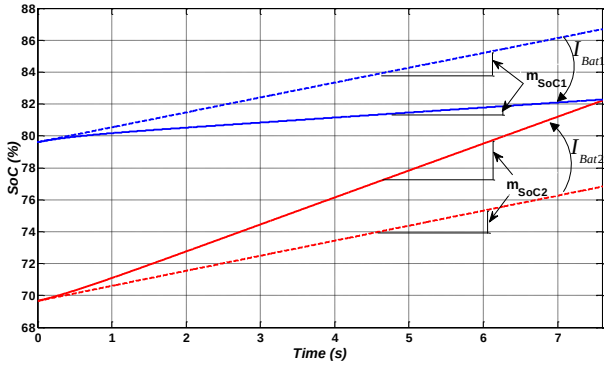

Fig. 6: Expected behavior of the equalization algorithm.

battery in (A/h), η_{Bati} is the charging/discharging efficiency, and $I_{Bati}(\tau)$ is the instantaneous current at each battery array [9]. In addition, the output current of each ESS (I_{ESSi}) is inversely proportional to the battery current (I_{Bati}) by a factor $1/D$,

$$I_{ESSi} = \frac{1}{D} I_{Bati} \quad (4)$$

where D is the duty-cycle of the PWM signal that controls the buck converter. By considering a constant current charge from (3), the following relationship can be obtained,

$$I_{ESSi} = -\frac{\Delta SoC_{Bati}(\%)}{\Delta t(s)} \left(\frac{3600 C_{Bati}(A/h)}{\eta_{Bati}(\%) D} \right) \quad (5)$$

where $\Delta SoC_{Bati} = SoC(\Delta t)_{Bati} - SoC(0)_{Bati}$. Then (5) takes the form:

$$I_{ESSi} = -m_{SoCi} K_{Bati} \tag{6}$$

being, m_{SoCi} the rate of the SoC, and K_{Bati} a proportionality constant that depends on the main parameters of the ESS.

In a general case, where n distributed active generators (PV+ESS) are integrated into the microgrid, it is easy to derive the Kirchhoff current law equation for the common node as:

$$\sum_{i=1}^{n} I_{ESSi} + \sum_{i=1}^{n} I_{RESi} - I_{Load} = 0 \tag{7}$$

where, (I_{Load}) is the load current, (I_{RESi}) is the power supplied for each RES, and (I_{ESSi}) is the current at each ESS.

In particular, for the proposed DC microgrid shown in Fig. 5, by combining (6) and (7), we have

$$\sum_{i=1}^{2} -m_{SoCi} K_{Bati} + \sum_{i=1}^{2} I_{RESi} - I_{Load} = 0 \tag{8}$$

Moreover, in order to perform the SoC equalization, it is required that the straight-line equations, that represents the behavior of the SoC within a defined period of time (Δt), are equalized between then as:

$$SoC(0)_{Bat1} + m_{SoC1}\Delta t = SoC(0)_{Bat2} + m_{SoC2}\Delta t \tag{9}$$

to be more precise $SoC(\Delta t)_{Bat1} = SoC(\Delta t)_{Bat2}$.

To get back to the point, the main task of the equalization algorithm is to solve the equation system composed by (8) and (9), in order to obtain the adequate values for m_{SoCi} that ensure the equalization of the SoC within a defined period (Δt). Once the value for each m_{SoCi} is obtained, it is necessary to obtain the adequate values for the weighting factor α_i (see (2)).

Firstly, the algorithm determines if the ESS' are being charged of discharged by evaluating the sign of any ESS current. This step is necessary since under the process of charge the smallest value of α should be assigned to the ESS whit the smallest SoC in order to charge the ESS with the smallest SoC faster. On the other hand, under the process of discharge the smallest value of α should be assigned to the ESS with the biggest SoC. In this way, the ESS with the biggest SoC will be discharged faster than the others. Consequently, it is also necessary to determine which ESS has the biggest SoC, this is possible by simple comparison. As a result, the values of α are bounded to 1. In addition, by considering differences at the capacity of distributed ESS the maximum value of the weighting factor (α_i) is determined by:

$$\alpha_{max} = C_{min}/C_{max} \tag{10}$$

where C_{max} and C_{min} are the maximum and minimum values of the ESS capacities. To illustrate, the algorithm is shown in Fig. 7.

Likewise, under normal operation it is expected a similar charge/discharge ratio for both ESS $(m_{SoC1} = m_{SoC2})$ despite of differences at the capacity of each ESS. To achieve this behavior, the virtual resistance Rd of the ESS with the biggest capacity should be weighted by the relationship C_{min}/C_{max}.

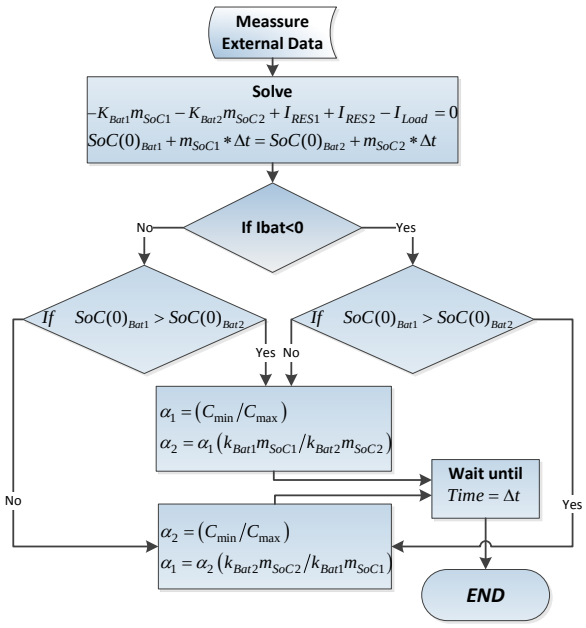

Fig. 7: Equalization algorithm.

TABLE I: Main Parameters of the microgrid

Parameter	Symbol	Value
Nominal Bus Voltage	V^*_{DC}	48 (V)
Nominal Load	R_{Load}	10 (Ω)
Maximum (RES) Power Rating	P_{RESmax}	300 W
Nominal Voltage	$Vbat$	48V
Nominal Battery Capacity	C_{bat}	0.02 (Ah)
Period of the Equalization Algorithm	Δt	5 (s)
Duty-cycle	D	0.93 (Ah)
Charging/discharging efficiency	η_{Bati}	100
Virtual Resistance	Rd	0.5 (Ω)

IV. Hardware-in-the-loop Results

The proposed equalization algorithm has been tested in a low voltage DC microgrid model established in a MATLAB/Simulink model that was downloaded into a dSPACE 1006 platform in order to evaluate the performance of the algorithm in real-time. The microgrid composition was presented in Fig. 5. The power stage and main parameters are presented in Table I. Particularly, small values of capacity ($C_{max} = 0.02$) have been selected in order to speed up the simulation time. Detailed models of the VRLA batteries have been used for simulation as is proposed in [15].

For the simulation, three main cases have been considered. That is, $C_{Bat1} = C_{Bat2}$, $C_{Bat2} > C_{Bat1}$, and $C_{Bat2} < C_{Bat1}$. All the cases were simulated by considering a total generation from RES of $P_{RES} = 260W$ and $P_{RES} = 100W$ for charging and discharging respectively.

A. Case $C_{Bat1} = C_{Bat2}$

Fig. 8 shows the performance of the equalization algorithm when the ESS are being charged. An initial SoC of 65% and 75% have been established for ESS1 and ESS2 respectively. Fig. 8(a) shows the equalization process for SoC_{Bat1} and SoC_{Bat2}. Fig. 8(b) shows the way the output current at each ESS is equally shared between ESS when the algorithm is not applied, and how the current is adjusted during the equalization in order to achieve the objective. At the end,

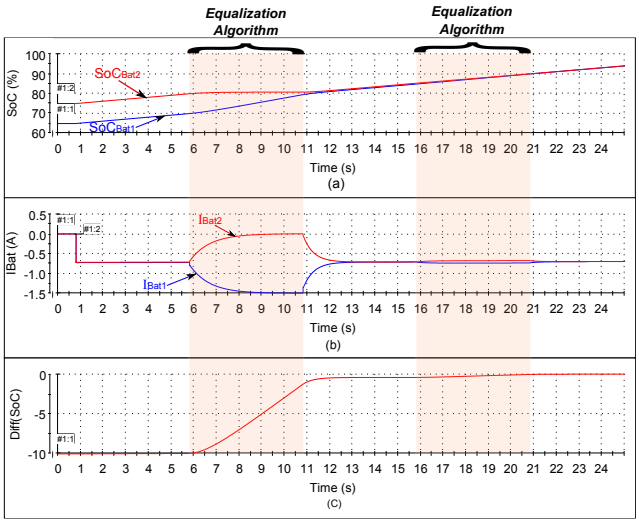

Fig. 8: ESS Charge when $C_{Bat1} = C_{Bat2}$: (a) SoC, (b) I_{Bat}, (c) Diff(SoC).

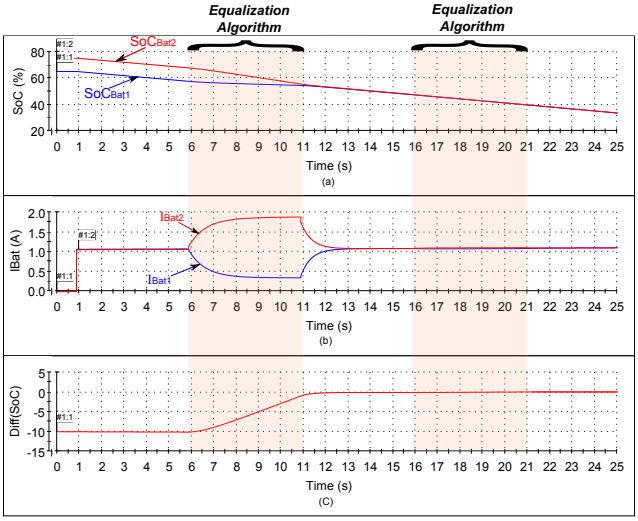

Fig. 9: ESS Discharge when $C_{Bat1} = C_{Bat2}$: (a) SoC, (b) I_{Bat}, (c) Diff(SoC).

Fig. 8(c) shows the difference between SoC $Diff(SoC) = SoC_{Bat1} - SoC_{Bat2}$, where it is possible to see that the difference is practically zero after two iterations. Similarly, Fig. 9 shows the response of the microgrid when the ESS' are being discharged. Comparing Fig. 8 and Fig. 9, we can see that for the discharging $|I_{Bat2}| > |I_{Bat1}|$, and for charging $|I_{Bat1}| > |I_{Bat2}|$ SoC equalization is achieved.

B. Case $C_{Bat2} > C_{Bat1}$

Fig. 10 and 11 show the response of the microgrid when $C_{Bat1} = 0.01(A/h)$. We can see that when the equalization is not applied, we have $|I_{Bat2}| > |I_{Bat1}|$. The reason of this is that ESS2 requires much more current in order to achieve $m_{SoC1} = m_{SoC2}$. However when the algorithm is applied, the current is adjusted in order to equalizing SoC's.

C. Case $C_{Bat2} < C_{Bat1}$

Fig. 12 and 13 show the response of the microgrid when $C_{Bat2} = 0.01(A/h)$. Compared to the previous case $|I_{Bat2}| < |I_{Bat1}|$, when the equalization is not applied. It is possible to

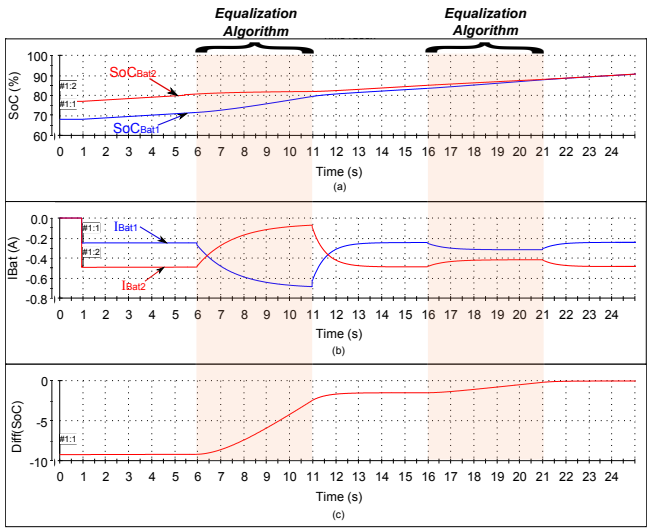

Fig. 10: ESS Charge when $C_{Bat1} < C_{Bat2}$: (a) SoC, (b) I_{Bat}, (c) Diff(SoC).

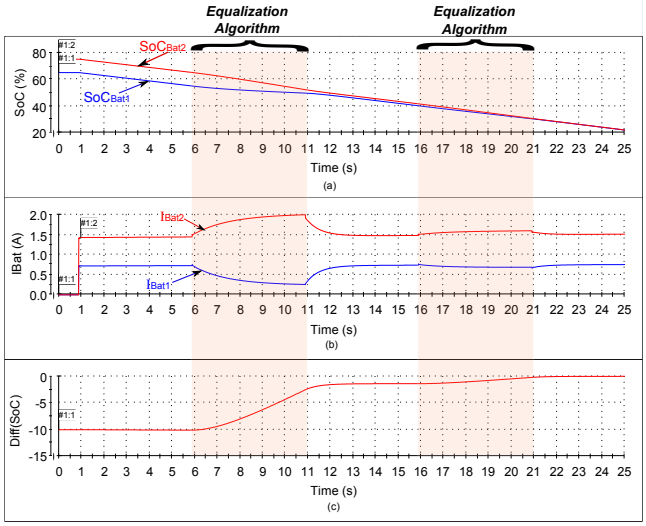

Fig. 11: ESS Discharge when $C_{Bat1} < C_{Bat2}$: (a) SoC, (b) I_{Bat}, (c) Diff(SoC).

see clearly from Fig. 12 (from $10s$ to $11s$), that the ESS is able to smoothly transfer from charge to discharge modes during the equalization process in order to achieve the goal.

V. Conclusion

The proposed been effective for SoC equalization in distributed ESS. Nevertheless, at least two iterations are required in order to equalize completely the SoC, This is because the transient and dynamic responses have not been considered by the algorithm. Despite this, and by assuming a linear behavior, the algorithm is able to equalize the SoC under few iterations. This algorithm can be complemented by an optimization process in order to minimize the period of time Δt, and by taking into account the power constrains of the system. Additionally, the algorithm can be easily adapted for AC microgrid and grid connected microgrids whit a larger number of interconnected active generators.

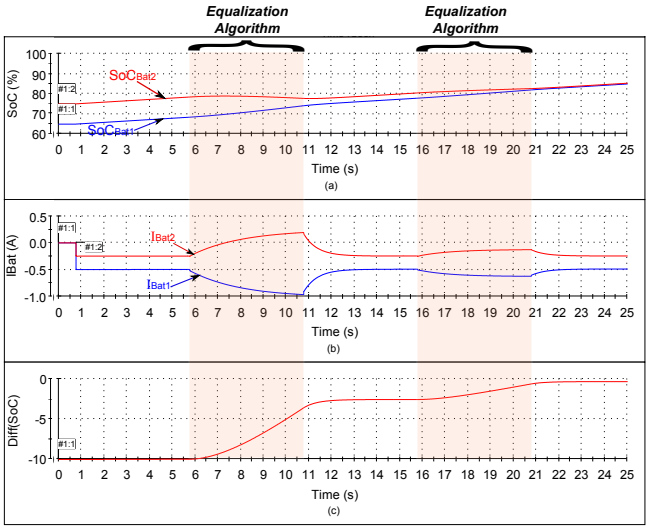

Fig. 12: ESS Charge when $C_{Bat1} > C_{Bat2}$: (a) SoC, (b) I_{Bat}, (c) Diff(SoC).

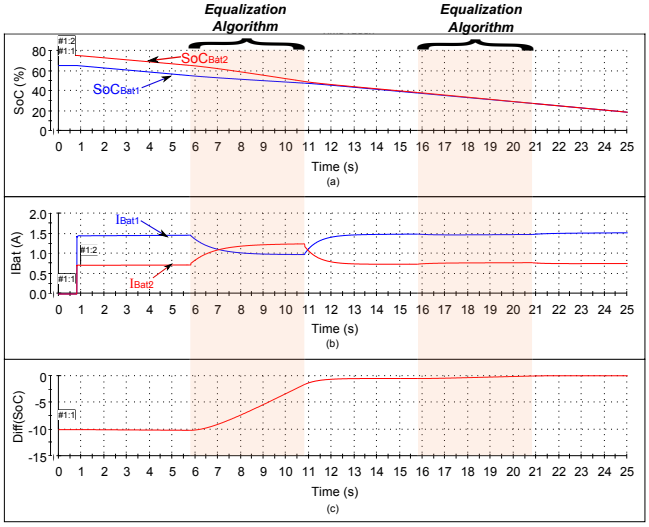

Fig. 13: ESS Discharge when $C_{Bat1} > C_{Bat2}$: (a) SoC, (b) I_{Bat}, (c) Diff(SoC).

REFERENCES

[1] W. Li, X. Mou, Y. Zhou, and C. Marnay, "On voltage standards for dc home microgrids energized by distributed sources," in *Power Electronics and Motion Control Conference (IPEMC), 2012 7th International*, vol. 3, pp. 2282–2286, 2012.

[2] D. McMenamin, "Case studies supporting -48 vdc as the power input of choice for computer equipment deployed in the telecom network," in *Telecommunications Energy Conference, 1998. INTELEC. Twentieth International*, pp. 261–265, 1998.

[3] C. Wang and P. Jain, "A quantitative comparison and evaluation of 48v dc and 380v dc distribution systems for datacenters," in *Telecommunications Energy Conference (INTELEC), 2014 IEEE 36th International*, pp. 1–7, Sept 2014.

[4] H. Kakigano, Y. Miura, and T. Ise, "Distribution voltage control for dc microgrids using fuzzy control and gain-scheduling technique," *Power Electronics, IEEE Transactions on*, vol. 28, no. 5, pp. 2246–2258, 2013.

[5] J. Guerrero, J. Vasquez, J. Matas, L. de Vicua, and M. Castilla, "Hierarchical control of droop-controlled ac and dc microgrids a general approach toward standardization," *IEEE Transactions on Industrial Electronics*, vol. 58, no. 1, pp. 158–172, 2011.

[6] H. Kanchev, D. Lu, F. Colas, V. Lazarov, and B. Francois, "Energy management and operational planning of a microgrid with a pv-based active generator for smart grid applications," *IEEE Transactions on Industrial Electronics*, vol. 58, pp. 4583–4592, Oct 2011.

[7] J. de Matos, F. e Silva, and L. Ribeiro, "Power control in ac isolated microgrids with renewable energy sources and energy storage systems," *IEEE Transactions on Industrial Electronics,*, vol. PP, no. 99, pp. 1–1, 2014.

[8] F. Marra, G. Yang, C. Traeholt, J. Ostergaard, and E. Larsen, "A decentralized storage strategy for residential feeders with photovoltaics," *IEEE Transactions on Smart Grid*, vol. 5, pp. 974–981, March 2014.

[9] . I. S. C. Committee, "Ieee guide for optimizing the performance and life of lead-acid batteries in remote hybrid power systems," 2008.

[10] D. Linden and T. Reddy, *Handbook of batteries*. McGraw-Hill handbooks, McGraw-Hill, 2002.

[11] Y.-K. Chen, Y.-C. Wu, C.-C. Song, and Y.-S. Chen, "Design and implementation of energy management system with fuzzy control for dc microgrid systems," *Power Electronics, IEEE Transactions on*, vol. 28, no. 4, pp. 1563–1570, 2013.

[12] J. Guerrero, J. Vasquez, J. Matas, M. Castilla, and L. de Vicuna, "Control strategy for flexible microgrid based on parallel line-interactive ups systems," *IEEE Transactions on Industrial Electronics*, vol. 56, no. 3, pp. 726–736, 2009.

[13] X. Lu, K. Sun, J. Guerrero, J. Vasquez, L. Huang, and R. Teodorescu, "Soc-based droop method for distributed energy storage in dc microgrid applications," in *Industrial Electronics (ISIE), 2012 IEEE International Symposium on*, pp. 1640–1645, 2012.

[14] Y. Zhang, H. J. Jia, and L. Guo, "Energy management strategy of islanded microgrid based on power flow control," in *Innovative Smart Grid Technologies (ISGT), 2012 IEEE PES*, pp. 1–8, 2012.

[15] T. Dragicevic, J. Guerrero, J. Vasquez, and D. Skrlec, "Supervisory control of an adaptive-droop regulated dc microgrid with battery management capability," *IEEE Transactions on Power Electronics*, vol. 29, no. 2, pp. 695–706, 2014.

[16] C. Li, T. Dragicevic, N. Diaz, J. Vasquez, and J. Guerrero, "Voltage scheduling droop control for state-of-charge balance of distributed energy storage in dc microgrids," in *Energy Conference (ENERGYCON), 2014 IEEE International*, pp. 1310–1314, May 2014.

[17] C. Li, T. Dragicevic, M. G. Plaza, F. Andrade, J. C. Vasquez, and J. M. Guerrero, "Multiagent based distributed control for state-of-charge balance of distributed energy storage in dc microgrids," in *Industrial Electronics Society, IECON 2014 - 40th Annual Conference of the IEEE*, pp. 2180–2184, Oct 2014.

[18] X. Lu, K. Sun, J. Guerrero, J. Vasquez, and L. Huang, "State-of-charge balance using adaptive droop control for distributed energy storage systems in dc microgrid applications," *IEEE Transactions on Industrial Electronics*, vol. 61, pp. 2804–2815, June 2014.

[19] Q. Shafiee, T. Dragicevic, J. Vasquez, and J. Guerrero, "Hierarchical control for multiple dc-microgrids clusters," *Energy Conversion, IEEE Transactions on*, vol. 29, pp. 922–933, Dec 2014.

[20] N. Diaz, T. Dragicevic, J. Vasquez, and J. Guerrero, "Intelligent distributed generation and storage units for dc microgrids - a new concept on cooperative control without communications beyond droop control," *IEEE Transactions on Smart Grid*, vol. 5, pp. 2476–2485, Sept 2014.

[21] J. Akerlund, "-48 v dc computer equipment topology-an emerging technology," in *Telecommunications Energy Conference, 1998. INTELEC. Twentieth International*, pp. 15–21, 1998.

[22] N. Diaz, A. Luna, and O. Duarte, "Improved mppt short-circuit current method by a fuzzy short-circuit current estimator," in *Energy Conversion Congress and Exposition (ECCE), 2011 IEEE*, pp. 211–218, Sept 2011.

[23] V. Salas, E. Olas, A. Barrado, and A. Lzaro, "Review of the maximum power point tracking algorithms for stand-alone photovoltaic systems," *Solar Energy Materials and Solar Cells*, vol. 90, no. 11, pp. 1555 – 1578, 2006.

[24] Y. Zhang, H. J. Jia, and L. Guo, "Energy management strategy of islanded microgrid based on power flow control," in *2012 IEEE PES Innovative Smart Grid Technologies (ISGT)*, pp. 1–8, Jan 2012.

[25] D. Wu, F. Tang, T. Dragicevic, J. Vasquez, and J. Guerrero, "Autonomous active power control for islanded ac microgrids with photovoltaic generation and energy storage system," *Energy Conversion, IEEE Transactions on*, vol. 29, pp. 882–892, Dec 2014.